DOI: 10.1002/ejic.200900284

Ternary Porphyrinato Hf^{IV} and Zr^{IV} Polyoxometalate Complexes

Alexander Falber,[a] Benjamin P. Burton-Pye,[a] Ivana Radivojevic,[a] Louis Todaro,[a] Raihan Saleh,[a] Lynn C. Francesconi,[a] and Charles Michael Drain*[a,b]

Dedicated to Professors Joyce Y. Corey and Lawrence Barton on the occasion of their retirement

Keywords: Porphyrinoids / Polyoxometalates / Photochemistry / Nanostructures

We report a facile, high-yield synthesis and characterization of discrete, ternary porphyrin–metal–polyoxometalate (por–M–POM) complexes where a group IV transition-metal ion is bound both to the porphyrin core and to the lacunary site of a Keggin POM, $PW_{11}O_{39}^{-7}$. The remarkably robust complexes exploit the fact that Hf^{IV} and Zr^{IV} are 7–8 coordinate and reside outside the plane of the porphyrin macrocycle, thus enabling the simultaneous coordination to *meso*-tetraphenylporphyrin (tpp) or *meso*-tetra(4-pyridyl)porphyrin (tpyp) and to the defect site in the Keggin framework. The physical properties of the (tpp)Hf($PW_{11}O_{39}$)$[tba]_5$, (tpyp)Hf($PW_{11}O_{39}$)$[tba]_5$, and (tpp)Zr($PW_{11}O_{39}$)$[tba]_5$ complexes are similar because the metal ions have similar oxidation states and coordination chemistry. This architecture couples the photonic properties of the porphyrin to the POM because the metal ion is incorporated into both frameworks. Thus, the ternary complexes can serve as a basis for the characterization of Hf^{IV} and Zr^{IV} porphyrins bound to oxide surfaces through the group IV metal ions. The Hf(por) and Zr(por) bind strongly to TiO_2 nanoparticles and indium tin oxide (ITO) surfaces, but significantly less binds to crystalline SiO_2 or TiO_2 surfaces. Together, the strong binding of the metalloporphyrins to the POM, nanoparticles, and the ITO surfaces, and paucity of binding to crystalline surfaces, suggests that the three-to-four open coordination sites on the Hf(por) and Zr(por) are predominantly bound at surface defect sites.

Introduction

Polyoxometalates (POMs) and porphyrins (por) are widely studied as components of functional materials, such as catalysts and photonics, because each possesses enormous potential for structural variation and tuning of their electronic properties. Porphyrins[1–6] and POMs[7–12] have been investigated for applications such as photovoltaics and supramolecular materials. There are numerous reports on the adsorption or attachment of porphyrins to a variety of surfaces using exocyclic motifs with a moiety designed to bond to the surface and a linker intervening between the macrocycle and the surface.[13–20] There are numerous supramolecular constructs of porphyrins and electron-acceptor species such as C_{60}.[21–26] In addition to POMs being good electron acceptors, in many ways the diverse photochemical, and coordination chemistry of porphyrins and POMs are complementary; therefore, robust complexes that photonically couple porphyrins and POMs should have unique properties. There are reports of films and other materials wherein cationic porphyrins and POMs are mixed;[27] for example, for catalysis,[28] an axially bound POM counterion on Mo^{V}(por),[29] two metalloporphyrins bridged by a POM bearing two nicotinamide moieties coordinated to the metal center,[30] and other porphyrin–POM structures,[31–33] but here we describe discrete ternary systems wherein a central metal ion is coordinated to *both* the por and a *defect* site in the lacunary POM. Previously, Keggin structures have been functionalized with cyclopentadienyl ligands at the lacunary site through Ti^{IV}, Zr^{IV}, and/or Hf^{IV} metal ions.[9,34,35] The recent report on the formation of Hf(por) dimers bridged by oxido ligands such as sulfate, phosphate, and peroxide indicates that multitopic counterions may serve as tectons to construct arrays of group IV metalloporphyrins.[36]

The three complexes reported herein are made in high yields from previously reported Zr^{IV} and Hf^{IV} porphyrinates[37] and the lacunary POM,[11] $H_3PW_{11}O_{39}^{4-}$ (Scheme 1): (tpp)Hf($PW_{11}O_{39}$)$[tba]_5$ (**1**), (tpyp)Hf($PW_{11}O_{39}$)$[tba]_5$ (**2**), and (tpp)Zr($PW_{11}O_{39}$)$[tba]_5$ (**3**). In contrast to the aforementioned systems, this nanoarchitecture enables photonic coupling of the two chelates mediated by the central metal ion. Because the chemistry of Zr^{IV} is

[a] Department of Chemistry and Biochemistry, Hunter College and Graduate Centre of the City University of New York, 695 Park Avenue, New York, NY 10065, USA
Fax: +1-212-772-5332
E-mail: cdrain@hunter.cuny.edu
[b] The Rockefeller University, 1230 York Avenue, New York, NY 10065, USA
Supporting information for this article is available on the WWW under http://dx.doi.org/10.1002/ejic.200900284.

generally similar to that of Hf^{IV}, the significantly greater natural abundance of Zr may make Zr(por) materials more cost effective if the functional properties are competitive.

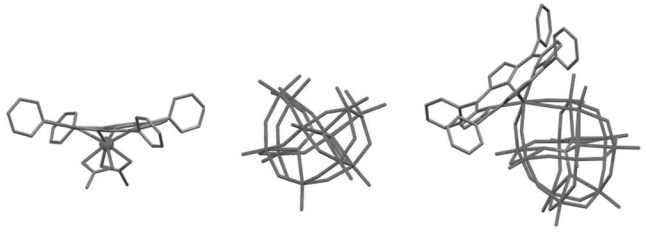

Scheme 1. Crystal structures of the starting (tpyp)Hf(OAc)$_2$ and ternary complex **2**; counterions were omitted for clarity. (i) to a solution of (tpyp)Hf(OAc)$_2$ in CH_2Cl_2/CH_3OH (1:1) was added $H_3PW_{11}O_{39}$[tba]$_4$ (1 equiv.) in CH_3CN with an excess amount of [tba]Br and 1% triethylamine (tea).

Since POMs are often regarded as good models for defect sites in oxide surfaces,[11] the crystal structure and physical properties of these ternary complexes suggested to us that one way to self-organize porphyrins onto oxide surfaces such that the photonic properties of the macrocycles are strongly coupled to the semiconductor is to use porphyrins coordinated to oxophilic group IV metals such as Hf and Zr. Indeed, when a variety of oxide particles, such as silica gel,[36] ITO, or TiO_2, are exposed to a solution containing the (por)Hf(L)$_2$ or (por)Zr(L)$_2$, where L = acetate or chloride, the spectroscopic signatures are observed to be similar to those of compounds **1**–**3**. While these group IV metalloporphyrins are strongly bound to the nanostructured surfaces, both scanning probe and reflectance data find a paucity of the complexes bound to crystalline TiO_2 and SiO_2 surfaces. Together, these data suggest that the three-to-four open metal ion coordination sites of the Hf(por)$^{2+}$ and Zr(por)$^{2+}$ are bound primarily to surface defect sites by displacement of the auxiliary acetate or chloride ligands.

Results and Discussion

Synthesis

Slowly adding a stoichiometric amount of the POM to solutions of (por)Hf(OAc)$_2$ or (por)Zr(OAc)$_2$[37] affords the por–M–POM complexes by displacement of the acetate ligands by the lacunary oxygen atoms of $H_3PW_{11}O_{39}$[tba]$_4$. Because the acidic protons from the POM can cause some demetalation of the porphyrin, the reaction must be buffered by a base such as triethylamine. In addition, the formal charge of the ternary complex is –5, requiring one additional equivalent of [tba]Br to be added to the mixture to yield the neutral (por)Hf($PW_{11}O_{39}$)[tba]$_5$ or (por)Zr($PW_{11}O_{39}$)[tba]$_5$ complexes. The chelating effect of the four oxygen atoms on the POM to the oxophilic Hf^{IV} or Zr^{IV} centers is strong, such that addition of more than one equivalent of POM can lead to porphyrin demetalation of the Hf complexes; most likely leading to the Hf($PW_{11}O_{39}$)$^{3-}$ or the corresponding dimer Hf($PW_{11}O_{39}$)$_2^{10-}$ complexes. Lacunary POMs chelated to lanthanide and group IV metal ions have been reported[38–41] (see Supporting Information). The (tpyp)Hf($PW_{11}O_{39}$)$^{5-}$ complex is somewhat more stable than the (tpp)Hf($PW_{11}O_{39}$)$^{5-}$ complex possibly due to electronic differences in the macrocycle or buffering effects of the pyridyl substituents.

Characterization

The formation of complexes **1**–**3** was monitored by UV/Vis absorption spectra of the porphyrinate portion of the complex (vide infra). Both the Soret and Q-band regions of the spectra display significant redshifts as the reaction progresses. The Soret bands at 412 and 414 nm for the (tpp)Hf(OAc)$_2$ and (tpyp)Hf(OAc)$_2$ complexes shift to 425 and 426 nm for the ternary complexes, respectively, whereas the major Q-band near 540 nm shifts to 550 and 548 nm. Similarly, the Soret band of (tpp)Zr(OAc)$_2$ is at 416 nm, whereas for compound **3** it is at 427 nm. As indicated by the NMR spectroscopic and crystal structure data, the redshifts arise from three interrelated effects: (a) a structural distortion in the porphyrin macrocycle,[42] (b) increasing N–Hf bond lengths, and (c) concomitant electronic coupling of the metalloporphyrin to the POM mediated by the group IV metal ion.[43] The POM encompasses a large portion of hafnium coordination sphere, drawing the metal center away from the porphyrin and sterically crowding the macrocycle (vide infra). Neither films formed by sequential dipping of these surfaces into solutions of the POM and cationic porphyrins, nor the axial coordinated porphyrin/POM materials exhibit substantial spectral changes relative to the metalloporphyrins.[27,29]

The ^{1}H NMR spectra of **1** and **3** (Figure 1, see Supporting Information for **2**) are highly diagnostic in comparison to those of the (por)M(OAc)$_2$ starting complexes (M = Hf or Zr). Proton assignments were confirmed by COSY 2D spectra and comparison of data between the three complexes. For the starting (por)M(OAc)$_2$ complexes, and for ternary complexes **1**–**3**, the *ortho* and *meta* ^{1}H NMR resonances on each phenyl substituent are not equivalent due to the asymmetry caused by the out-of-plane M^{IV} ion binding. For complexes **1**–**3** there is a nonparallel geometry between the porphyrin macrocycle and the mean O_4 plane of the POM lacunary oxygen atoms (see crystallographic analysis), further segregating the phenyl substituents into two types: nearer to and further from the POM. Thus, the four porphyrin phenyl groups display a total of 10 distinct resonances for **1** and **3**, and 8 for **2**. This analysis is also supported by the well-resolved resonances for the pyrrole protons. The distortion of the macrocycle is indicated by the large shift of the *ortho* protons on the opposite side of the porphyrin; for example, (tpp)Hf(POM) is shifted to ca. 9.25 and 9.55 ppm because they are now tilted inward towards the ring current as found with the (por)M(OAc)$_2$ starting materials and lanthanide M(por)$_2$ sandwich com-

plexes.[44,45] The ^1H NMR spectra of the (tpyp)Hf-$(PW_{11}O_{39})$[tba]$_5$ complex is very similar showing eight distinct aryl resonances and four pyrrolic resonances similar to those found with the tpp ternary complex. ^{31}P NMR for all three ternary complexes display a singlet peak between –16.20 and –16.30 ppm, which is comparable to the cyclopentadienyl analogue, (cp)Hf$(PW_{11}O_{39})$[tba]$_4$, which displays a peak at –12.3 ppm.[34]

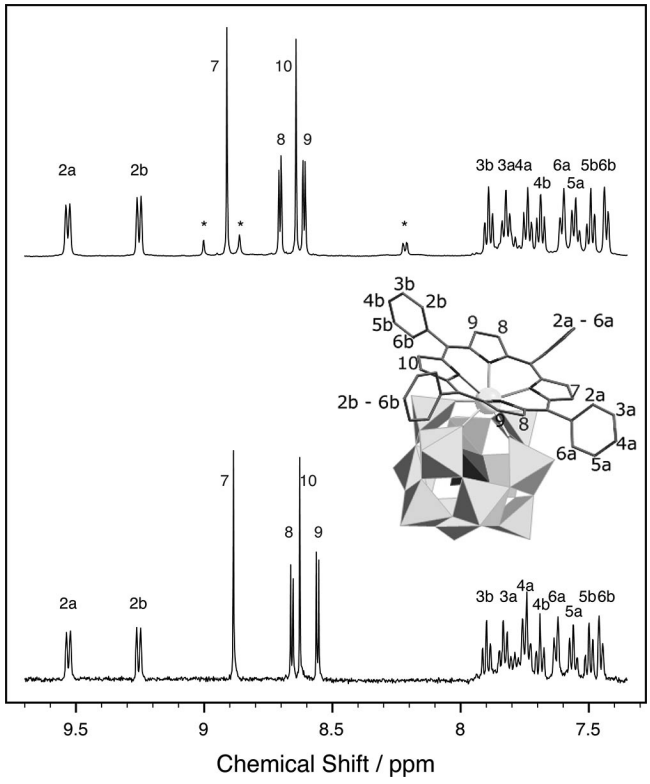

Figure 1. 500 MHz ^1H NMR of compound **1** (top) and **3** (bottom) in CD_3CN; * indicates a small amount of the starting Hf(tpp)OAc_2 material.

The five tba counterions are cleanly observed in the NMR spectra of all three complexes, as are small quantities of the tea buffer. The underlying resonances in the phenyl region can be attributed to other conformations of the complexes and are not consistent with starting materials or decomposition. Variable-temperature NMR experiments reveal that there are other accessible conformations of the phenyl groups in the (por)Zr$(PW_{11}O_{39})$[tba]$_5$ complex. The phenyl resonances significantly sharpen at elevated temperatures and become more complex at lower temperatures (35 and 0 °C, respectively). The interconversion and equilibriums between conformations in distorted metalloporphyrins have been studied,[42] but the differences seem to be largely relegated to the aryl moieties in this case. Note that since the 3a, 4a, 3b, 4b resonances (Figure 1) are mostly impacted, it is possible that subtle dynamical differences in the tilt toward the macrocycle or the aryl–porphyrin dihedral angle cause the observed spectra. Likely conformational differences based on the crystal structure are not obvious, but local minima in the rotation of the porphyrin relative to the POM seem unlikely.

Crystallography

The X-ray crystal structure of the (tpyp)Hf$(PW_{11}O_{39})^{5-}$ complex was obtained (Figure 2). Only two tba units are found for every (tpyp)Hf$(PW_{11}O_{39})^{5-}$, which indicates that the charge balance is accounted for, in part, by protonation and/or highly disordered tba. There are channels with disordered solvent molecules, but the large number of metal atoms and the refinement of data from several crystals yields similar results, which assures the accuracy of the structure of the ternary complex. Formally, the crystal structure is of (tpyp)Hf$(PW_{11}O_{39})$[tba]$_2H_3^+$. This protonation may occur on the pyridyl groups themselves acting as a built in buffer system for the acidic complex and be another reason for the greater stability of the (tpyp)Hf-$(PW_{11}O_{39})^{-5}$ complex.

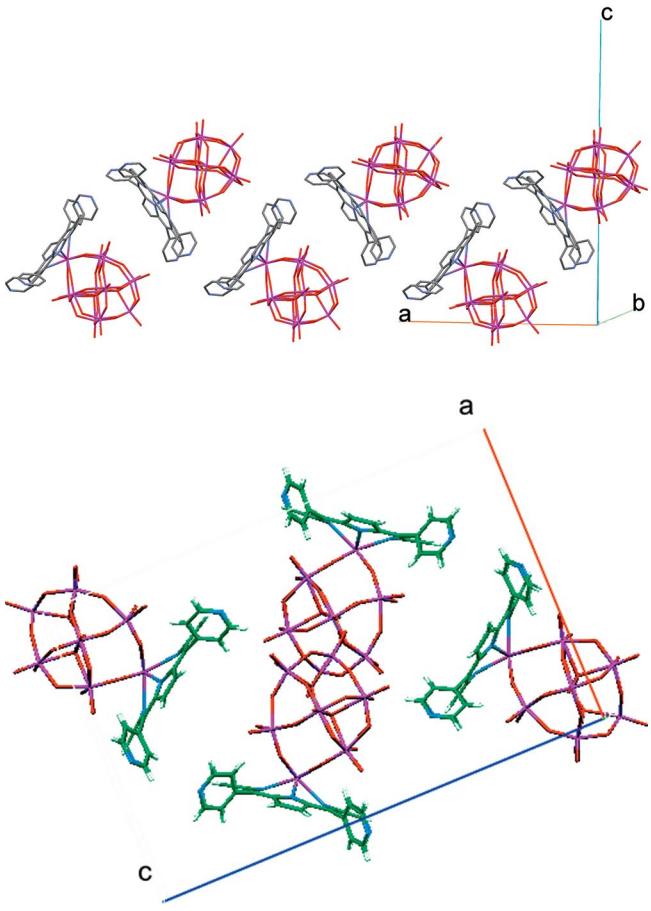

Figure 2. Two views of the crystal packing of the (H_3tpyp)Hf-$(PW_{11}O_{39})$[tba]$_2$ complex; protons, counterions, and solvent are omitted for clarity (see Supporting Information).

The entire coordination around the hafnium ion assumes an antiprismatic geometry where the N_4 plane of the porphyrin and the O_4 plane of the lacunary site form the two square faces. There is a 3.1° dihedral angle between the mean N_4 and O_4 planes; thus, the porphyrin is tilted towards the POM on one side, which gives rise to the distinctive ^1H NMR spectra. The structure of the Hf(tpyp)

portion of ternary complex **2** shows that the porphyrin core adopts a saddle-type distortion and the four inner pyrrole N atoms deviate from the C_{20} macrocycle towards the Hf ion, which lies above it. The distance of the hafnium atom from the mean N_4 plane is 1.22 Å, which is notably longer than the 1.04 Å deviation measured for the (tpyp)Hf-$(OAc)_2$ complex. The average N–Hf bond length is 2.34 Å compared to 2.26 Å for the acetate derivative,[46] further illustrating the affect of the POM on the hafnium coordination to the porphyrin core. The structure of the $PW_{11}O_{39}^{7-}$ portion of the complex is similar to previously reported structures of zirconium and hafnium Keggin and Wells–Dawson POMs.[34,41] The monovacant POM binds to the hafnium asymmetrically, deviating from the mean O_4 plane by 1.14 Å. The Hf–O bond varies between 2.20 and 2.15 Å, which is nearly identical to the reported $Hf(PW_{11}O_{39})_2^{10-}$ dimer complex,[41] indicating that the POM lacunary site binds the hafnium ion similarly. There is no detectable structural perturbation in the POM as a result of the adjoining tetrapyrrole system.

The tertiary structure of the $(tpyp)Hf(PW_{11}O_{39})^{5-}$ crystal is comprised of the complex forming zig–zag chains along the *a* axis where the top surface of one porphyrin approaches the side of the POM of an adjacent complex (Figure 2). The porphyrin core is in line with the hafnium ion of the neighboring complex at an angle of approximately 78°. The pattern repeats itself every two units along the chain, over a distance of 9.42 Å. When viewing down the *a* axis, large channels containing disordered solvent, water, and counterions are observed between the chains of the ternary complexes. Unexpectedly, there are no direct interporphyrin interactions and the organization of the complex in the crystal is mediated by pyridyl H-bonds to water and solvent molecules.

Hf(tpp) and Zr(tpp) on Oxide Surfaces

Since the POM is a good model of oxide surfaces[11] and the exchange of the acetate ligands on the $(por)M(OAc)_2$ complexes for the lacunary site on the POM is facile, the protruding Hf^{IV} and Zr^{IV} ions may be a good way to attach tetraarylporphyrins to oxide surfaces such as ITO, SiO_2, SnO_2, and TiO_2. The use of metal ions that protrude from the macrocycle as a mode of attaching the chromophore to the oxide surfaces differs from the many organic moieties that are used to tether porphyrins.[13–20,47,48] The significant changes in the optical spectra (Figure 3) between the $(por)M(OAc)_2$ and ternary complex indicate good electronic coupling between the porphyrin and the POM.[49] To evaluate surface binding, drop casting or dipping a glass substrate or glass with an ITO coating, with a root mean square (rms) roughness of <1 nm, results in robust binding of $Zr(tpp)^{2+}$ and $Hf(tpp)^{2+}$ to the surface. The metalloporphyrin does not wash off with vigorous rinsing with toluene or other solvents, but can be removed with alcohols or organic acids, which further indicates binding by the oxophilic metal ions. UV/Vis absorption spectra reveal that more of the $Zr(tpp)^{2+}$ and $Hf(tpp)^{2+}$ complexes bind piranha-cleaned glass than ozone-cleaned glass, because the former leaves more hydroxyl groups on the surface than the latter;[50] note that they are similar to the ternary complexes (Figure 3).

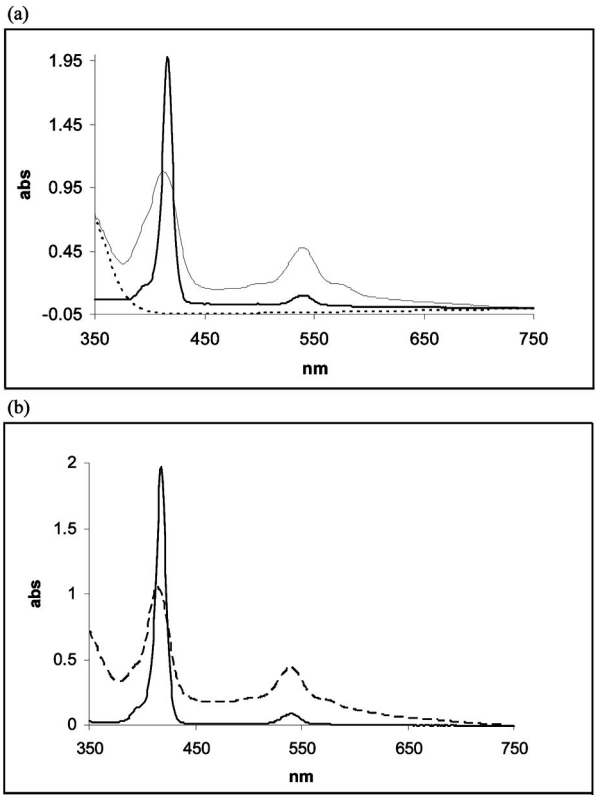

Figure 3. (a) UV/Vis spectra of $(tpp)Hf(OAc)_2$ in toluene (solid line), reflectance spectrum of a ca. 1 mm film of TiO_2 nanoparticles coated with $(tpp)Hf(OAc)_2$ (dashed line) and an untreated TiO_2 film (dotted line); (b) UV/Vis spectra of $(tpp)ZrHf(OAc)_2$ in toluene (solid line), reflectance spectrum of a ca. 1 mm film of TiO_2 nanoparticles coated with $(tpp)Zr(OAc)_2$ (dashed line). The dynamic range of the reflectance-integrating sphere is ca. one absorbance unit.

Stirring a slurry of ca. 5 nm particles of TiO_2 in a 0.5 mM solution of $(tpp)M(OAc)_2$, or Hf or Zr metalloporphyrin complexes with other anionic ligands such as Cl^-, in dry toluene for a minimum of 2 h effectively binds the chromophore to this material as well (Figure 4). The rate of binding to the surface is proportional to the lability of the auxiliary anionic ligands ($Cl^- > HPO_4^{2-} > OAc^-$). The metalloporphyrin is not removed from the TiO_2 by washing with toluene and the slurries are readily cast onto glass or ITO for analysis. The charge balance can be accommodated by either deprotonation of hydroxyl groups on the surface or the presence of the anionic ligands in the vicinity. After similar incubation of crystalline SiO_2 and TiO_2 surfaces with the $Hf(tpp)^{2+}$ complex and rinsing, very little metalloporphyrin is observed by using AFM and UV/Vis reflectance. The (tpp)M(POM) ternary complex, the tight binding of the Hf and Zr tpp complexes to nanopowders of silica and TiO_2, the minimal binding to crystalline SiO_2 surfaces, and the results on glass are all indications that Hf(por) and

Zr(por) prefer to bind to defect sites and those with a greater surface density of hydroxyl groups (see Supporting Information for a model).

Figure 4. (Top) Slurries of TiO_2 nanoparticles with left to right: tpp, (tpp)$Zr(OAc)_2$, Zn(tpp), and (tpp)$Hf(OAc)_2$. 30 mg of TiO_2 nanoparticles were treated with 0.5 mM porphyrin solution (2 mL) by mixing slurry overnight, removing the solvent, and rinsing with toluene (2 or 3 times). (Bottom) Powders on upper row from left: tpp, Zn(tpp), and (tpp)$Zr(OAc)_2$; lower row from left: tcpp (thf used as solvent and for rinse) and (tpp)$Hf(OAc)_2$.

The diffuse reflectance UV/Vis spectra of all surface-bound systems are similar to the ternary complexes in solution, but the redshifts in the Soret bands near 410 nm are somewhat less (Figure 3, Supporting Information). The smaller redshift likely indicates that the group IV metal ion is not pulled out of the macrocycle to the same extent relative to the POM when bound to the surface. This is expected because the lacunary site of the POM is in an optimal geometry for Hf or Zr binding. The broadened optical spectra are typical of surface bound dyes. While the fluorescence intensity of the (por)$Hf(OAc)_2$ and (por)$Zr(OAc)_2$ is diminished due to the heavy atom effect, it is further quenched in the ternary complexes and when the $Zr(tpp)^{2+}$ and $Hf(tpp)^{2+}$ are bound to the ITO surfaces. The fluorescence is not similarly quenched when the (por)M complexes strongly adsorbs to glass. After similar binding and rinsing of the particles, UV/Vis reflectance spectra show that free base and Zn^{II} tpp adsorb onto these substrate to a much smaller extent but exhibit much greater fluoresce intensities.[51] The widely studied tetracarboxyphenylporphyrin (tcpp) also remains on the TiO_2. AFM studies of the compound on the ITO do not reveal large aggregates of the metalloporphyrin and a somewhat decreased rms roughness. Because the $Zr(tpp)^{2+}$ and $Hf(tpp)^{2+}$complexes robustly bind surfaces, likely at defect sites and we remove unbound materials, the surface coverages are much less than the coating of porphyrins such as tetracarboxyphenyl derivatives on ITO or TiO_2 surfaces by chemisorption.[16,17,20,52] Relative to the surface, the horizontal orientation of the Zr and Hf complexes of tpp also diminishes the maximum potential coverage compared to the vertical orientation of the tcpp.[52] Thus, the optical cross sections in the visible region for the materials with Hf and Zr porphyrins on TiO_2 and on ITO are smaller than the absorbed coatings. These electrochemical and photonic studies are ongoing and will be published elsewhere.

Conclusions

The matching of metal ion size and coordination chemistry to the binding properties of two significantly different ligands, one organic and one inorganic, affords an avenue for the formation of new (por)M(POM) hybrid materials in high yields. These complexes exploit the light absorbing and photonic properties of porphyrinic systems directly coupled to the complementary photonic and structural properties of POMs through simultaneous multidentate coordination of a single metal ion. The efficiency of charge transport from molecules into semiconductors underpins a variety of hybrid molecular-semiconductor device architectures and other photonic materials. Charge transport efficiency is mediated by appropriate matching of molecular HOMO–LUMO gaps to semiconductor bandgaps, the linker, and the proximity of the molecule.[2,17,18,20,51] Metals that axially bind oxygen, for example, Ti, and Sn, and Mo, may also allow porphyrin attachment to oxide surfaces, but intervening tethers are needed for *meso* tetraarylporphyrins, because these metal ions reside near the porphyrin plane and the orthogonal aromatic moieties inhibit direct metal–surface interactions. Therefore, these (por)M(POM) materials may serve as a new platform to study the fundamental properties porphyrinoids attached to oxide surfaces through group IV metals.[16,53] The properties of the ternary complexes, and by inference those on the surfaces, arise because the Hf and Zr ions are coordinated by *both* the lacunary POM and the porphyrin.

Experimental Section

Instrumentation and Reagents: All UV/Vis spectra and diffuse reflectance spectra were taken in 1-cm quartz or glass cuvettes in

CH_2Cl_2 with a Carey Bio 3 spectrophotometer unless otherwise indicated. Mass spectrometry was done as a service by the University of Illinois, Urbana-Champaign or with an Agilent 1100 LC/MSD instrument. NMR spectra were run with a 500 MHz Varian Inova and chemical shifts (ppm) are referenced to the proton solvents. A Joel 400 MHz NMR instrument was used for ^{31}P spectra. Fluorescence spectra were taken with a Spex Tau-3 fluorometer in 1-cm quartz cuvettes in right-angle mode. X-ray data were collected with a Nonius Kappa CCD. Gasses, reagents, and solvents were used as received unless otherwise noted. $HfCl_4$ and $Hf(cp)_2Cl_2$ were obtained from Strem Chemicals. Porphyrins were obtained from Aldrich or from Frontier Scientific. All solvents and other reagents were from Aldrich Disposable vials and test tubes were used once. Titanium(IV) oxide (TiO_2), nanopowder, 99.7%, anatase was purchased from Aldrich. ITO-coated glass slides were purchased from Aldrich, and the glass cover slips were purchased from Fisher. The hafnium and zirconium porphyrinate starting materials, (tpp)Hf(OAc)$_2$ (tpyp)Hf(OAc)$_2$, and (tpp)Zr(OAc)$_2$, and the corresponding derivatives with two chloride counterions, were synthesized according to literature methods,[37,54,55] as was the free-base lacunary Keggin polyoxometalate, $H_3PW_{11}O_{39}[tba]_4$.[56] Mass spectrometric and IR and NMR spectroscopic data of the starting materials are consistent with previous reports, and the spectroscopy of the ternary complexes are consistent with crystal structure data found for (tpp)Hf($PW_{11}O_{39}$)[tba]$_5$ (Supporting Information).

***meso*-Tetraphenylporphyrinatohafnium(IV)$PW_{11}O_{39}$ Tetrabutylammonium Salt {(tpp)Hf($PW_{11}O_{39}$)[tba]$_5$}:** Hf(tpp)(OAc)$_2$ (20 mg, 0.022 mmol, 910 g mol^{-1}) was dissolved in CH_2Cl_2/CH_3OH (1:1, 10 mL) in a 18 × 150 mm test tube with a magnetic stir bar at room temperature. $H_3PW_{11}O_{39}[tba]_4$ (76 mg, 0.021 mmol, 3650 g mol^{-1}) and [tba]Br (5 mg) was dissolved separately in acetonitrile (5 mL) containing 1% v/v triethylamine. The resulting clear POM solution was added dropwise over the course of 5 min to the stirring hafnium porphyrinate solution. The reaction was monitored by UV/Vis spectroscopy, where the presence of the ternary complex was signified by a large redshift in the porphyrin Soret band from 414 to 425 nm, over the course of 1 h. The solvent was then removed under vacuum, and the residue was dissolved in a minimum amount of CH_2Cl_2 (ca. 4 mL) and filtered to remove a small amount of insoluble salts. The product was precipitated with hexanes (25 mL) and collected on a glass filter. The product was allowed to dry initially in air and then under vacuum without heat to yield (tpp)Hf($PW_{11}O_{39}$)[tba]$_5$ (91 mg, 98%). IR (nujol, NaCl): $\tilde{\nu}$ = 1100–700, 1063 (m, br.), 958 (m), 890 (w), 816 (s, br.) 723 (m) cm^{-1}. UV/Vis (CH_2Cl_2): λ (log ε) = 403 (4.51), 425 (5.53), 508 (3.40), 548 (4.21), 583 (3.30) nm. ^1H NMR (CD_3CN, 30 °C): δ = 9.53 (d, J = 7.58 Hz, 2 H, phen-*o*), 9.25 (d, J = 7.64 Hz, 2 H, phen-*o*), 8.91 (2 H, pyrrole), 8.71 (d, J = 4.65 Hz, 2 H, pyrrole), 8.64 (s, 2 H, pyrrole), 8.61 (d, J = 4.58 Hz, 2 H, pyrrole), 7.89 (t, J = 7.61 Hz, 2 H, phen-*m*), 7.82 (t, J = 7.46 Hz, 2 H, phen-*m*), 7.75 (t, J = 7.49 Hz, 2 H, phen-*p*), 7.69 (t, J = 7.49 Hz, 2 H, phen-*p*), 7.60 (d, J = 7.46 Hz, 2 H, phen-*o*), 7.55 (t, J = 7.40 Hz, 2 H, phen-*m*), 7.49 (t, J = 7.46 Hz, 2 H, phen-*m*), 7.43 (d, J = 7.58 Hz, 2 H, phen-*o*), 3.12 (m, 40 H, N-CH_2-), 1.61 (m, 40 H, -CH_2-), 1.38 (m, 40 H, -CH_2-), 0.98 (t, J = 7.34 Hz, 60 H, -CH) ppm. ^{31}P NMR (CD_3CN): δ = –16.29 ppm. MS (ESI–): m/z = 1726.4 [(tpp)Hf($PW_{11}O_{38}$)$^{-2}$].

***meso*-Tetraphenylporphyrinatozirconium(IV)$PW_{11}O_{39}$ Tetrabutylammonium Salt {(tpp)Zr($PW_{11}O_{39}$)[tba]$_5$}:** Prepared by following the same method as that used to prepare the hafnium complex but by using (tpp)Zr(OAc)$_2$ as the starting material. Yield: 82 mg, 81%. IR (KBr disc): $\tilde{\nu}$ = 1100–700, 1054 (m, br.), 954 (s), 890 (w), 826 (s, br.) 745 (m) cm^{-1}. UV/Vis (CH_2Cl_2): λ (log ε) = 404 (4.01), 427 (4.84), 509 (3.059), 548 (3.60), 586 (2.77) nm. ^1H NMR (CD_3CN, 30 °C): δ = 9.53 (d, J = 7.34 Hz, 2 H, phen-*o*), 9.25 (d, J = 7.34 Hz, 2 H, phen-*o*), 8.89 (2 H, pyrrole), 8.66 (d, J = 4.40 Hz, 2 H, pyrrole), 8.63 (s, 2 H, pyrrole), 8.56 (d, J = 4.89 Hz, 2 H, pyrrole), 7.90 (t, J = 7.82 Hz, 2 H, phen-*m*), 7.83 (t, J = 7.83 Hz, 2 H, phen-*m*), 7.74 (t, J = 8.07 Hz, 2 H, phen-*p*), 7.69 (t, J = 7.34 Hz, 2 H, phen-*p*), 7.63 (d, J = 7.84 Hz, 2 H, phen-*o*), 7.56 (t, J = 7.83 Hz, 2 H, phen-*m*), 7.50 (t, J = 7.59 Hz, 2 H, phen-*m*), 7.45 (d, J = 7.82 Hz, 2 H, phen-*o*), 3.16 (m, 40 H, N-CH_2-), 1.66 (m, 40 H, -CH_2-), 1.41 (m, 40 H, -CH_2-), 1.00 (t, J = 7.34 Hz, 60 H, -CH_3) ppm. ^{31}P NMR (CD_3CN): δ = –16.30 ppm. MS (TOF–): m/z = 1933.4822 ($PW_{11}O_{39}ZrC_{44}H_{28}N_4[C_{16}H_{36}N]_2[H]^{2-}$; +2.32 ppm), 1812.8449 ($PW_{11}O_{39}ZrC_{44}H_{28}N_4[C_{16}H_{36}N]_1[H]_2^{2-}$; +20.95 ppm), 1208.2313 ($PW_{11}O_{39}ZrC_{44}H_{28}N_4[C_{16}H_{36}N]_1[H]^{3-}$; +24.28 ppm), 1127.8054 ($PW_{11}O_{39}ZrC_{44}H_{28}N_4H_2^{3-}$; +78.65 ppm).

***meso*-Tetra(4-pyridyl)porphyrinatohafnium(IV)$PW_{11}O_{39}$ Tetrabutylammonium Salt {(tpyp)Hf($PW_{11}O_{39}$)[tba]$_5$}:** A similar procedure to that described above was followed: (tpyp)Hf(OAc)$_2$ (20 mg, 0.022 mmol, 914 g mol^{-1}) was stirred with $H_3PW_{11}O_{39}[tba]_4$ (75 mg) and [tba]Br (5 mg). The reaction was complete after 20 min of stirring. The product was isolated by precipitating the target complex with hexanes (15 mL) from a CH_2Cl_2 solution (5 mL) to yield (tpyp)Hf($PW_{11}O_{39}$) [tba]$_5$ (90 mg; 97%). IR (nujol, NaCl): $\tilde{\nu}$ = 1100–700, 1133 (w), 1076 (sh.), 1054 (s), 949 (s), 880 (m), 806 (vs. br.), 749 (sh.) cm^{-1}. UV/Vis (CH_2Cl_2): λ (log ε) = 402 (4.42), 426 (5.41), 505 (3.42), 550 (4.21), 582 (3.44) nm. ^1H NMR (CD_3CN, 30 °C): δ = 9.50 (br. s, 2 H, py-*o*), 9.18 (d, J = 4.2 Hz, 2 H, py-*o*), 9.08 (d, J = 7.2 Hz, 2 H, py-*m*), 9.02 (d, J = 4.2 Hz, 2 H, py-*m*), 8.94 (s, pyrrole), 8.78 (br. d, J = 8.1 Hz, 4 H, pyrrole and py-*m* overlap), 8.71 (br. d, J = 8.1 Hz, 4 H, pyrrole and py-*m* overlap), 8.68 (s, 2 H, pyrrole), 7.64 (br. s, 2 H, py-*o*), 7.47 (d, J = 6.1 Hz, py-*o*), 3.14 (m, 40 H, N-CH_2-), 1.64 (m, 40 H, -CH_2-), 1.41 (m, 40 H, -CH_2-), 0.99 (t, J = 7.34 Hz, 60 H, -CH_3) ppm. ^{31}P NMR (CD_3CN): δ = –16.25 ppm. MS (ESI–): m/z = 3444.1 [(tpyp)Hf($PW_{11}O_{37}$)$^{-1}$], 1728.7 [(tpyp)Hf($PW_{11}O_{38}$)$^{-2}$]. Suitable crystals for X-ray diffraction were obtained for the (tpyp)-Hf($PW_{11}O_{39}$)$^{-5}$ complex. The complex (50 mg) was dissolved in CH_3CN/CH_3OH (1:1, 5 mL) in an 18 × 150 mm test tube with a magnetic stir bar. Diethyl ether was added by pipette while stirring until the solution appeared cloudy. The solution was then placed in a warm water bath to evaporate just enough of the ether to make the solution almost clear of particulates. The solution was capped and placed in a freezer at –10 °C for 4 d, after which time long, dark purple needles collected on the sides and bottom of the test tube. The structure revealed this material to be (tpyp)Hf-($PW_{11}O_{39}$)[tba]$_2H^+_3$

Single-Crystal X-ray Diffraction: The intensity data for **2** were measured with a Bruker–Nonius KappaCCD diffractometer (graphite-monochromated Mo-K_α radiation, λ = 0.71073 Å, ϕ-ω scans) at 100(2) K (Table 1). The data were not corrected for absorption. Details of the solution and refinements for this compound are presented below: The crystal of **2**, with approximate dimensions 0.18 × 0.18 × 0.30 mm, were orthorhombic with space group *Pnma*. The final unit-cell constants of **2** were a = 19.419(4) Å, b = 27.157(5) Å, c = 29.642(6) Å, V = 15632(5) Å^3, Z = 4, ρ = 1.976 g cm^{-1}, μ = 8.80 mm^{-1}, formula weight = 4649.55. The structure of **2** was solved with SHELXS-97 and refined by full-matrix least-squares on F^2 with SHELXL-97. The hydrogen atoms were included in the structure-factor calculations, but their parameters were not refined. The final discrepancy indices for the 18158 reflections (θ < 27.50°) were R = 0.0912 (calculated on F) and R_w = 0.2076 (calculated on F^2) with 730 parameters varied. The final difference map peaks <3.16 e Å^{-3} are near the heavy atoms, haf-

nium and tungsten. CCDC-717412 contains the supplementary crystallographic data for this paper. These data can be obtained free of charge from The Cambridge Crystallographic Data Centre via www.ccdc.cam.ac.uk/data_request/cif.

Table 1. Crystallographic data for (tpyp)Hf($PW_{11}O_{39}$)[tba]$_2H_3$.

Empirical formula	$C_{117}H_{177}HfN_{15}O_{39}PW_{11}$
Formula mass	4649.55
System	orthorhombic
Space group	*Pnma*
Unit cell	15632.(5)
a / Å	19.419(4)
b / Å	27.157(5)
a / Å	29.642(6)
β / °	90
γ / °	90
Volume / Å^3	90
Z	4
$\rho_{calcd.}$ / mg cm^{-3}	1.976
μ(Mo-K_α) / mm^{-1}	8.798
T / K	100(2)
F(000)	8788
Crystal size / cm	$0.3 \times 0.18 \times 0.18$
range / °	1.73 to 27.50
Index ranges	$-14 \le h \le 25$
	$-33 \le k \le 35$
	$-38 \le l \le 31$
Data/restraints/parameters	18158/19/730
Final *R* indices [$I > 2\sigma(I)$]	
R_1	0.0912
wR_2	0.2076
R indices (all data)	
R_1	0.1752
wR_2	0.1720
Largest diff. peak and hole / e Å^{-3}	3.158 and –1.669
Selected bond lengths / Å	
Hf–N	2.328–2.358
Hf–O	2.206–2.151
W–$O_{lacunary}$	1.755–1.784
W–$O_{bridging}$	1.847–2.087
W=O	1.679–1.723
Hf – mean plane of N_4	1.220
Hf – mean plane of O_4	1.144

Binding of Hf(por) and Zr(por) to Glass, ITO, and TiO_2 Surfaces: All glass and ITO substrates were cleaned in an ozone cleaner (20 min) or by a piranha solution (NH_4OH/H_2O_2, 3:1; 30 min) followed by rinsing with copious amounts of water just prior to use. A drop of ca. 4 μM solution of the (tpp)Hf(OAc)$_2$ or (tpp)Zr(OAc)$_2$ in dry toluene was placed on the substrate and allowed to dry in air. Alternatively, the substrate was dipped in a ca. 0.4 mM solution for 1 h. After drying, all substrates were washed with toluene to remove any unbound materials. For TiO_2, (tpp)Hf(OAc)$_2$ (0.8 mg) or (tpp)Zr(OAc)$_2$ was dissolved in distilled toluene (2 mL) and titanium(IV) oxide nanopowder (ca. 30 mg), 99.7% anatase with average size 5 nm (Aldrich) was added to the solution. After sonicating for 5 min, the slurry was stirred overnight. The slurry was then centrifuged for 5 min to separate the coated particles, which are a pink color due to attachment of Hf(tpp)$^{2+}$ or Zr(tpp)$^{2+}$ on TiO_2. Similar treatment of the TiO_2 particles with Zn(tpp) and tpp in control experiments resulted in most of the porphyrin remaining in solution. The solution was decanted, the coated particles were rinsed with toluene (2 to 3 times) to remove unbound materials, and left to dry in air.

Supporting Information (see footnote on the first page of this article): Further experimental details; UV/Vis, IR, ^{1}H, COSY, and ^{31}P NMR spectra; mass spectrometry; structures with solvent molecules included; scheme with hypothesized binding of the Hf and Zr porphyrins to a TiO_2 surface.

Acknowledgments

This work was supported by the US National Science Foundation (NSF) (CHE-0554703 to C. M. D.), AP Fellows Program (DGE-0231800 for support of A. F. and IGERT DGE-9972892). C. M. D. acknowledges support from the Israel-United States Binational Science Foundation. Hunter College Chemistry infrastructure is supported by the NSF, the National Institutes of Health, (including RCMI G12-RR-03037), and the City University of New York.

[1] a) S. Cherian, C. C. Wamser, *J. Phys. Chem. B* **2000**, *104*, 3624–3629; b) J. Hao, A. Giraudeau, Z. Ping, L. Ruhlmann, *Langmuir* **2008**, *24*, 1600–1603; c) J. Hao, Y. Xia, L. Wang, L. Ruhlmann, Y. Zhu, Q. Li, Y. Wei, *Angew. Chem.* **2008**, *120*, 2666–2670.
[2] Y. Tachibana, S. A. Haque, I. P. Mercer, J. R. Durrant, D. R. Klug, *J. Phys. Chem. B* **2000**, *104*, 1198–1205.
[3] C. M. Drain, G. Bazzan, T. Milic, M. Vinodu, J. C. Goeltz, *Isr. J. Chem.* **2005**, *45*, 255–269.
[4] C. M. Drain, X. Chen in *Encyclopedia of Nanoscience & Nanotechnology* (Ed.: H. S. Nalwa), American Scientific Press, New York, **2004**, vol. 9, pp. 593–616.
[5] T. N. Milic, N. Chi, D. G. Yablon, G. W. Flynn, J. D. Batteas, C. M. Drain, *Angew. Chem. Int. Ed.* **2002**, *41*, 2117–2119.
[6] C. M. Drain, F. Nifiatis, A. Vasenko, J. D. Batteas, *Angew. Chem. Int. Ed.* **1998**, *37*, 2344–2347.
[7] O. Dmitrenko, W. Huang, T. E. Polenova, L. C. Francesconi, J. A. Wingrave, A. V. Teplyakov, *J. Phys. Chem. B* **2003**, *107*, 7747–7752.
[8] J. E. Toth, F. C. Anson, *J. Am. Chem. Soc.* **1989**, *111*, 2444–2451.
[9] J. F. W. Keana, M. D. Ogan, *J. Am. Chem. Soc.* **1986**, *108*, 7951–7957.
[10] J. F. W. Keana, M. D. Ogan, Y. LU, M. Beer, J. Varkey, *J. Am. Chem. Soc.* **1986**, *108*, 7957–7963.
[11] D. E. Katsoulis, *Chem. Rev.* **1998**, *98*, 359–388.
[12] D. L. Long, E. Burkholder, L. Cronin, *Chem. Soc. Rev.* **2007**, *36*, 105–121.
[13] C. M. Drain, G. Smeureanu, J. Batteas, S. Patel in *Dekker Encyclopedia of Nanoscience and Nanotechnology* (Eds.: J. A. Schwartz, C. I. Contescu, K. Putyera), Marcel Dekker, Inc., New York, **2004**, vol. 5, pp. 3481–3502.
[14] D. E. Barlow, L. Scudiero, K. W. Hipps, *Langmuir* **2004**, *20*, 4413–4421.
[15] J. Otsuki, S. Kawaguchi, T. Yamakawa, M. Asakawa, K. Miyake, *Langmuir* **2006**, *22*, 5708–5715.
[16] M. K. Nazeeruddin, R. Hunphry-Baker, D. L. Officer, W. M. Campbell, A. K. Burrell, M. Graetzel, *Langmuir* **2004**, *20*, 6514–6517.
[17] J. R. Stromberg, A. Marton, H. L. Kee, C. Kirmaier, J. R. Diers, C. Muthiah, M. Taniguchi, J. S. Lindsey, D. F. Bocian, G. J. Meyer, D. Holten, *J. Phys. Chem. C* **2007**, *111*, 15464–15478.
[18] Y.-H. Chan, A. E. Schuckman, L. M. Perez, M. Vinodu, C. M. Drain, J. D. Batteas, *J. Phys. Chem. C* **2008**, *112*, 6110–6118.
[19] M. Tanaka, S. Hayashi, S. Eu, T. Umeyama, Y. Matano, H. Imahori, *Chem. Commun.* **2007**, 2069–2071.
[20] J. Rochford, D. Chu, A. Hagfeldt, E. Galoppini, *J. Am. Chem. Soc.* **2007**, *129*, 4655–4665.
[21] A. Varotto, L. Todaro, M. Vinodu, J. Koehne, G.-y. Liu, C. M. Drain, *Chem. Commun.* **2008**, 4921–4923.

[22] L. H. Tong, J.-L. Wietor, W. Clegg, P. R. Raithby, S. I. Pascu, J. K. M. Sanders, *Chem. Eur. J.* **2008**, *14*, 3035–3044.
[23] F. Marorri, D. Bonifazi, R. Gehrig, J.-L. Gallani, F. Diederich, *Isr. J. Chem.* **2005**, *45*, 303–319.
[24] K. Tashiro, T. Aida, *Chem. Soc. Rev.* **2007**, *36*, 189–197.
[25] T. Hasobe, K. Saito, P. V. Kamat, V. Troiani, H. Qiu, N. Solladie, K. S. Kim, J. K. Park, D. Kim, F. D'Souza, S. Fukuzumi, *J. Mater. Chem.* **2007**, *17*, 4160–4170.
[26] F. D'Souza, M. E. El-Khouly, A. L. McCarty, S. Gadde, P. A. Karr, M. E. Zandler, Y. Araki, O. Ito, *J. Phys. Chem. B* **2005**, *109*, 10107–10114.
[27] G. Bazzan, W. Smith, L. C. Francesconi, C. M. Drain, *Langmuir* **2008**, *24*, 3244–3249.
[28] I. C. M. S. Santos, S. L. H. Rebelo, M. S. S. Balula, R. R. L. Martins, M. M. M. S. Pereira, M. M. Q. Simoes, M. G. P. M. S. Neves, J. A. S. Cavaleiro, A. M. V. Cavaleiro, *J. Mol. Catal. A* **2005**, *231*, 35–45.
[29] A. Yokoyama, T. Kojima, K. Ohkubo, S. Fukuzumi, *Chem. Commun.* **2007**, 3997–3999.
[30] C. Allain, S. Favette, L.-M. Chamoreau, J. Vaissermann, L. Ruhlmann, B. Hasenknopf, *Eur. J. Inorg. Chem.* **2008**, 3433–3441.
[31] D. Hagrman, P. J. Hagrman, J. Zubieta, *Angew. Chem. Int. Ed.* **1999**, *38*, 3165–3168.
[32] A. Tsuda, E. Hirahara, Y.-S. Kim, H. Tanaka, T. Kawai, T. Aida, *Angew. Chem. Int. Ed.* **2004**, *43*, 6327–6331.
[33] C. M. Drain, A. Varotto, I. Radivojevic, *Chem. Rev.*, DOI: 10.1021/cr8002483.
[34] L. M. Babcock, *Synthesis and Characterization of Group 4 Organometal Oxide Complexes*, University of Illinois, Urabana-Champaign, **1988**.
[35] H. J. Kim, S. Jung, Y. M. Jeon, D. Whang, K. Kim, *Chem. Commun.* **1997**, 2201–2202.
[36] A. Falber, L. Todaro, I. Goldberg, M. V. Favilla, C. M. Drain, *Inorg. Chem.* **2008**, *47*, 454–467.
[37] H. J. Kim, D. Whang, K. Kim, Y. Do, *Inorg. Chem.* **1993**, *32*, 360–362.
[38] Q. Luo, R. C. Howell, J. Bartis, M. Dankova, J. W. DeW. Horrocks, A. L. Rheingold, L. C. Francesconi, *Inorg. Chem.* **2002**, *41*, 6112–6117.
[39] Q.-H. Luo, R. C. Howell, M. Dankova, J. Bartis, C. W. Williams, J. W. DeW. Horrocks, J. Victor, G. Young II, A. L. Rheingold, L. C. Francesconi, M. R. Antonio, *Inorg. Chem.* **2001**, *40*, 1849–1901.
[40] A. J. Gaunt, I. May, D. Collison, O. D. Fox, *Inorg. Chem.* **2003**, *42*, 5049–5051.
[41] C. N. Kato, A. Shinohara, K. Hayashi, K. Nomiya, *Inorg. Chem.* **2006**, *45*, 8108–8119.
[42] C. M. Drain, S. Gentemann, J. A. Roberts, N. Y. Nelson, C. J. Medforth, S. Jia, M. C. Simpson, K. M. Smith, J. Fajer, J. A. Shelnutt, D. Holten, *J. Am. Chem. Soc.* **1998**, *120*, 3781–3791.
[43] T. Yamase, *Chem. Rev.* **1998**, *98*, 307–326.
[44] J. W. Buchler, M. Nawra, *Inorg. Chem.* **1994**, *33*, 2830–2837.
[45] E. M. Davoras, C. A. Spyroulias, E. Mikros, A. C. Coutsolelos, *Inorg. Chem.* **1994**, *33*, 3430–3434.
[46] J. L. Huhmann, J. Y. Corey, N. P. Rath, C. F. Campana, *J. Organomet. Chem.* **1996**, *513*, 17–26.
[47] J. Rochford, E. Galoppini, *Langmuir* **2008**, *24*, 5366–5374.
[48] H. Imahori, H. Norieda, Y. Nishimura, I. Yamazaki, K. Higuchi, N. Kato, T. Motohiro, H. Yamada, K. Tamaki, M. Arimura, Y. Sakata, *J. Phys. Chem. B* **2000**, *104*, 1253–1260.
[49] D.-C. Lee, G. M. Morales, Y. Lee, L. Yu, *Chem. Commun.* **2006**, 101–102.
[50] J. Batteas, J. Helt, C. Xu, M. Weldon, *ANTEC 2001 Proceedings: Materials* **2001**, *2*, 1951–1954.
[51] A. Hagfeldt, M. Grätzel, *Acc. Chem. Res.* **2000**, *33*, 269–277.
[52] W. M. Campbell, K. W. Jolley, P. Wagner, K. Wagner, P. J. Walsh, K. C. Gordon, L. Schmidt-Mende, M. K. Nazeeruddin, Q. Wang, M. Grätzel, D. L. Officer, *J. Phys. Chem. C* **2007**, *111*, 11760–11762.
[53] M. K. Nazeeruddin, C. Klein, P. Liska, M. Grätzel, *Coord. Chem. Rev.* **2005**, *249*, 1460–1467.
[54] The structure of the Hf(tpyp)OAc_2 complex is similar to that reported for the Hf(tpp)OAc_2 complex. J. L. Huhmann, N. P. Rath, J. Y. Corey, *Acta Crystallogr., Sect. C: Cryst. Struct. Commun.* **1996**, *52*, 2486–2488.
[55] S. Ryu, D. Whang, J. Kim, W. Yeo, K. Kim, *J. Chem. Soc., Dalton Trans.* **1993**, 205–209.
[56] E. Radkov, R. H. Beer, *Polyhedron* **1995**, *14*, 2139–2143.

Received: March 27, 2009
Published Online: May 7, 2009

